Vol. 590: 19–34, 2018
https://doi.org/10.3354/meps12432

MARINE ECOLOGY PROGRESS SERIES
Mar Ecol Prog Ser

Published March 12

Microbial food web connections and rates in a subtropical embayment

K. E. Selph[1,*], E. Goetze[1], M. J. Jungbluth[1,3], P. H. Lenz[2], G. Kolker[1]

[1]Department of Oceanography, University of Hawai'i at Mānoa, Honolulu, Hawai'i 96822, USA
[2]Pacific Biosciences Research Center, University of Hawai'i at Mānoa, Honolulu, Hawai'i 96822, USA

[3]*Present address:* Romberg Tiburon Center for Environmental Sciences, San Francisco State University, Tiburon, California 94920, USA

ABSTRACT: Kāne'ohe Bay, Hawai'i, USA, an oligotrophic subtropical coastal embayment, is a stable ecosystem dominated by picophytoplankton through most of the year (dry state). After heavy rains, macronutrients from high stream flow result in elevated phytoplankton biomass and change the community to one dominated by diatoms (wet state). However, the effect of this perturbation on the overall productivity of the community, in particular linkages between lower trophic levels and planktonic metazoan consumers, is unknown. Given that microzooplankton are the main intermediaries between phytoplankton and higher trophic levels, this study examined phytoplankton growth and mortality rates using microscopy and flow cytometry, in conjunction with seawater dilution experiments during wet and dry system states. During low stream flow (dry state), *Synechococcus* dominated the phytoplankton, with growth rates of 1.1 ± 0.4 d^{-1}, and pico- to nano-sized autotrophic eukaryotes were either growing slowly or dying. Growth increased rapidly in experimental bottles with macronutrient (ammonium and phosphorus) addition. Sixty percent of *Synechococcus* were consumed daily, whereas autotrophic eukaryote mortalities (0.5 d^{-1}) greatly exceeded their growth rates. Microzooplankton were dominated by <30 µm oligotrich ciliates and gymnodinoid dinoflagellates. During the wet state, autotrophic biomass doubled, but microzooplankton biomass increased ~7-fold, including large increases in naupliar and larval stages of metazoans. During wet conditions, the path from primary producers to metazoan consumers had fewer trophic levels and episodically increased the overall productivity of the bay over the dry system state.

KEY WORDS: Phytoplankton · Microzooplankton · Grazing rates · Growth rates · Subtropical coastal embayment

INTRODUCTION

Microzooplankton grazers, including 2–200 µm protists, copepod nauplii and larval meroplankton, are the primary consumers of phytoplankton in all marine ecosystems, including coastal areas (Sherr & Sherr 2002, Calbet & Landry 2004, Schmoker et al. 2013). However, microzooplankton diversity varies among communities and depends on the taxa and size of the dominant phytoplankton, which in turn directly affects trophic linkages and overall ecosystem productivity. Oligotrophic coastal ecosystems in subtropical and tropical areas are typically dominated by very small phytoplankton taxa (Bienfang & Takahashi 1983, Hopcroft & Roff 1990, Furnas 2007), indicating that the microzooplankton community is composed of multiple trophic levels (Reckermann & Veldhuis 1997, Calbet & Landry 1999, First et al. 2009). Perturbations to these ecosystems occur on many scales, from localized nutrient inputs to changes in circulation (Böttjer & Morales 2005, Cox et al. 2006, Chen et al. 2009). The effects of these changes on the micro-

*Corresponding author: selph@hawaii.edu

bial food web have been little studied, especially in comparison with temperate and high-latitude coastal communities (Schmoker et al. 2013). Understanding these perturbations is important, as they affect trophic pathways and overall productivity.

Kāne'ohe Bay, Hawai'i, USA, a subtropical embayment on the island of O'ahu, is representative of coastal oligotrophic habitats and is characterized by event-scale perturbations in the phytoplankton community driven by sporadic inputs of nutrients following storms (Cox et al. 2006, Hoover et al. 2006). The shallow southern bay (~9.5 m average depth) is situated between oligotrophic subtropical waters (offshore, ~3 km away from the middle of the bay) and the urban watershed. After episodic rainfall, which marks the transition from dry to wet ecosystem states, the coastal watershed introduces nutrients through stream runoff and groundwater discharge, resulting in a higher-nutrient ecosystem (Ringuet & Mackenzie 2005, Cox et al. 2006, Drupp et al. 2011). Prior research has determined macronutrient concentrations before and following storms (Stimson 2015), characterized variability in phytoplankton biomass and productivity in the bay (Bienfang & Takahashi 1983, Taguchi & Laws 1987, 1989), and described the abundance and feeding relationships of the mesozooplankton (Kimmerer 1984, Calbet et al. 2000, Scheinberg et al. 2005). However, few studies have reported on the phytoplankton and microzooplankton taxa and on how these change with ecosystem state (wet vs. dry), thereby supporting higher or lower ecosystem productivity.

The focus of this study was to relate phytoplankton community dynamics to microzooplankton community structure and grazing impact under stable (oligotrophic, dry) and storm-perturbed (wet) ecosystem states. Specifically, the main objective was to understand if microbial community structure and associated population dynamics change as a result of wet vs. dry ecosystem states and episodically funnel more productivity to metazoan consumers. To approach this question, the seawater dilution experiments in the present study describe the phytoplankton and microzooplankton community in Kāne'ohe Bay under stable (oligotrophic, dry) conditions, as well as when the bay is episodically impacted by elevated nutrient inputs (wet conditions).

MATERIALS AND METHODS

Field sampling dates and location

Samples were collected for seawater dilution experiment incubations during 3 sampling periods: March 2012 (2 sample dates), August 2012 (2 sample dates), and between 27 May and 5 June 2013 (5 sample dates). Samples were taken in the late morning from surface waters in southern Kāne'ohe Bay (21° 25′ 56.7″ N, 157° 46′ 47.1″ W) (Fig. 1).

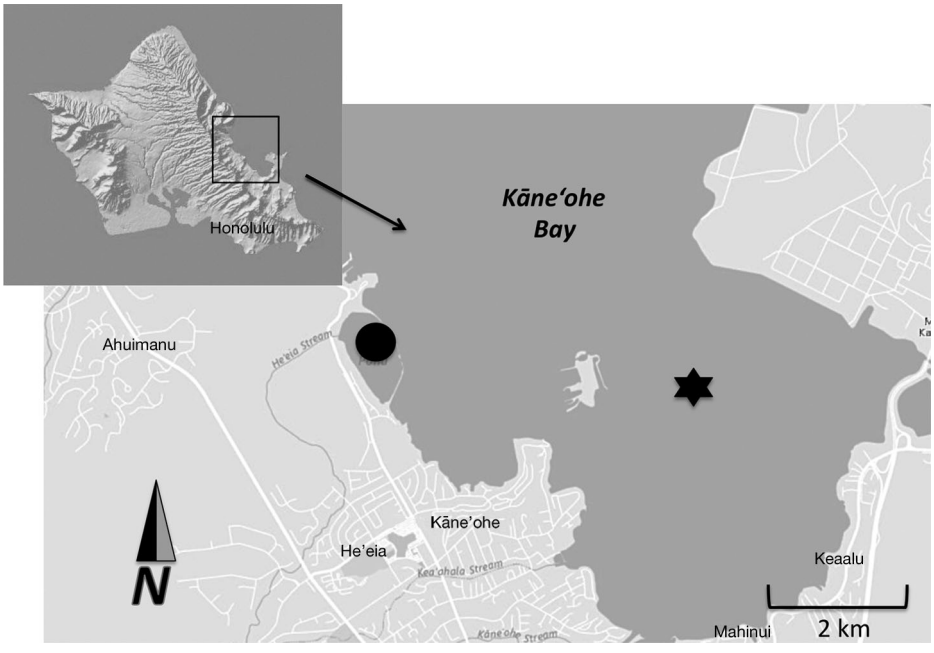

Fig. 1. O'ahu, Hawai'i, USA, with inset box indicating Kāne'ohe Bay. The sampling station location in the southern bay is indicated with a star, and the location of He'eia Stream input to the bay is indicated with a dot. The map was generated using tools available at www.arcgis.com

Environmental parameters

Photosynthetically active radiation (µmol m^{-2} s^{-1}) and wind direction and speed (knots) measurements were obtained from the Hawai'i Institute of Marine Biology's weather station on Coconut Island (21.433° N, 157.7863° E, http://oos.soest.hawaii.edu/erddap/index.html). Rainfall (mm) from stream discharge data in the 2 wk prior to sampling were obtained from the He'eia Stream gauge (http://nwis.waterdata.usgs.gov/nwis/), one of the 5 streams flowing into Kāne'ohe Bay (Fig. 1).

Chl *a* was estimated by filtration of seawater onto 25 mm GF/F filters, frozen in liquid nitrogen and stored at −80°C. Frozen filters were extracted (24 h, dark, −20°C) with 90% acetone and analyzed using a Turner Designs 10AU fluorometer, calibrated with the Welschmeyer (1994) method. Because of unexplained degradation of the chl *a* signal, no data were available for Expts 1 and 2, so the phaeopigment signature was used as a proxy for the minimum chl *a* present in these experiments.

Microbial abundance and biomass

Flow cytometry (FCM) samples stained with Hoechst 34442 (1 µg ml^{-1}, final concentration) (Campbell & Vaulot 1993, Monger & Landry 1993, Campbell et al. 1994) were analyzed with a Beckman-Coulter Altra flow cytometer. Particle signals collected were scatter, DNA, phycoerythrin and chl *a* and were analyzed using FlowJo (Tree Star). Carbon biomass was estimated using 32, 200 and 10 fg C $cell^{-1}$ for *Prochlorococcus* (PRO), *Synechococcus* (SYN) and heterotrophic (non-pigmented) bacteria (H-BACT), respectively (Christian & Karl 1994, Garrison et al. 2000, Buitenhuis et al. 2012). For autotrophic eukaryotes (A-EUK), the average biomass (1550 fg C $cell^{-1}$) of the 2–3 µm phytoplankton obtained from epifluorescence microscopy (EPI-MICRO) was used, since most of the cells were in this size category.

Abundance and biomass of nano- and microplankton by EPI-MICRO were preserved using 0.4% paraformaldehyde, stained with 0.5 nM proflavin, and then filtered onto 0.8 or 8 µm black polycarbonate filters (Midland Scientific). Filters were stained with 50 µg l^{-1} DAPI, mounted and frozen (−80°C) until analysis. Slide images were taken with Microfire software (ver. 1.1) using an Olympus U-LH100H-GAPO digital color camera attached to an Olympus Model BX51 TRF epifluorescence microscope. Thirty random fields were chosen for 3 sequential micrographs using filter sets for chl *a*, phycoerythrin and DNA, and images were analyzed with Zeiss imaging software (ver. 3.0, Media Cybernetics). Biovolumes (prolate spheroid, assuming width = height) were converted to carbon biomass, using biomass (pg C $cell^{-1}$) = 0.216 × $biovolume^{0.939}$ for non-diatoms and biomass (pg C $cell^{-1}$) = 0.288 × $biovolume^{0.811}$ for diatoms (Menden-Deuer & Lessard 2000).

Ciliates, dinoflagellates and metazoan larvae and nauplii were preserved in dark bottles with a 1/20 dilution of acid Lugol's solution (Throndsen 1978) and analyzed using the Utermöhl technique (Sherr & Sherr 1993), with digital images (Moticam camera) taken for dimensional analyses using Motic Images Plus software (inverted microscopy of acid Lugol's preserved samples [LUGOLS-MICRO] technique). Biovolume was estimated from cellular length and width, along with the geometric formulae for the closest approximate shape (e.g. sphere, prolate spheroid, cone, ½ sphere + cone). Biovolume was converted to biomass, using biomass (pg C $cell^{-1}$) = 0.216 × $biovolume^{0.939}$ (Menden-Deuer & Lessard 2000). Metazoan larvae and nauplii biomass (average of ≥3 independent samples) was estimated using length equations (Almeda et al. 2011, see Table 2).

Incubation experiments for rate measurements

Surface water phytoplankton growth rates and microzooplankton grazing rates were determined from 9 experiments (Expts 1–9) using the seawater dilution method (Landry & Hassett 1982, Selph et al. 2005). Seawater dilution series were prepared in pre-washed (10% HCl, plus 3 rinses with ambient 0.1 µm seawater) polycarbonate bottles (1120 ml), using 0.1 µm filtered seawater (Pall AcroPak 500 capsule with Supor Membrane, pre-soaked in 10% HCl for ≤1 h) and whole seawater (WSW), resulting in duplicate bottles filled with 20, 38, 55, 82 and 100% WSW, with nutrients added (45 µM NH_4Cl and 31.5 µM KH_2PO_4, final concentration) to relieve potential nutrient limitation. Additional duplicate WSW control bottles (no nutrients added) were prepared. Ambient nitrogen and phosphorus concentrations in Kāne'ohe Bay were much lower than those used in the nutrient-addition treatments. These treatments are used to encourage maximum phytoplankton growth rates to ensure that lack of remineralized nutrients are not a problem in estimation of mortality rates, rather than estimating *in situ* growth rates, so the amount of nutrient addi-

tion is not a crucial feature in interpreting these experiments.

Bottles were incubated in clear plexiglass incubators placed at ~1 m depth, to simulate *in situ* light and temperature conditions, for 24 h. Initial and final samples were taken for FCM, chl *a*, abundance and biomass of the microbial community (EPI-MICRO, LUGOLS-MICRO).

The phytoplankton net growth rate (k, d^{-1}) was plotted as a function of seawater dilution factor. The dilution factor (D_i) is the proportion of WSW in the dilution treatment for the nutrient-enriched treatments and yields phytoplankton growth (μ_N, growth with nutrients = y-axis intercept) and phytoplankton mortality due to microzooplankton grazing (m = slope) (Landry & Hassett 1982). A Model II linear regression was calculated (Bohonak & van der Linde 2004) and a t-test was applied ($p < 0.05$) to test the significance of the result (H_0: $m = 0$). Chl *a*-based mortality rates (m, d^{-1}) and ciliate abundance (C, cells l^{-1}) were used to estimate ciliate clearance rates (F, µl ciliate^{-1} h^{-1}), i.e. $F = C \times m$.

Phytoplankton growth without added nutrients (μ_0) is the sum of grazing mortality (m) and mean net growth rate (k_0) in the unamended seawater treatments ($\mu_0 = k_0 + m$). Growth rates were adjusted for photoadaptation, by determining the average red fluorescence per cell in the initial (red_i) and final (red_f) SYN and A-EUK (FCM) populations and computing a weighted average correction factor, CF = $\ln(red_f/red_i)$, to add to the chl *a*-based growth rate. Ciliate and dinoflagellate (heterotrophs only) mortality (m_Z) and gross growth (μ_Z) rates were estimated from initial and final estimates of their biomass in 20 and 100% WSW bottles, using the following:

$$m_Z = (k_{20\%} - k_{100\%})/(1 - 0.20) \quad (1)$$

and

$$\mu_Z = k_{100\%} + m_Z \quad (2)$$

where $k_{20\%}$ and $k_{100\%}$ equal the net growth rate in the 20 and 100% incubation bottles, respectively. This approach assumes that growth and grazing of the heterotrophs are decoupled by dilution in a linear fashion and that heterotroph gross growth rates are unaffected by dilution.

RESULTS

Environmental context

Based on stream discharge rates, each experiment was categorized as occurring under either wet, high flow (>0.05 m^3 s^{-1}) or dry, normal flow (<0.05 m^3 s^{-1}) conditions (Fig. 2, Table 1). The microbial ecosystem reflected in Expts 1 and 2 represented wet conditions, with elevated chl *a* of ≥0.7 µg l^{-1}. The August 2012 experiments (Expts 3 and 4) were preceded by normal stream flows (<0.05 m^3 s^{-1}) and reflect dry conditions, with chl *a* of ≤0.5 µg l^{-1}. Expt 5 (27 May 2013) was preceded by a week of normal stream flow (<0.05 m^3 s^{-1}), but on 12 May, stream discharge was 0.5 m^3 s^{-1} before rapidly returning to normal stream flow (Fig. 2). On 28 May (between sampling for Expts 5 and 6), another large pulse of water entered the bay (1.3 m^3 s^{-1}), but chl *a* (~0.3 µg l^{-1}) was still low on 29 or 31 May (Expts 6 and 7). Thus, Expts 6 and 7 represent a transition from dry to wet conditions in Expts 8 and 9 (chl *a* ≥0.9 µg l^{-1}).

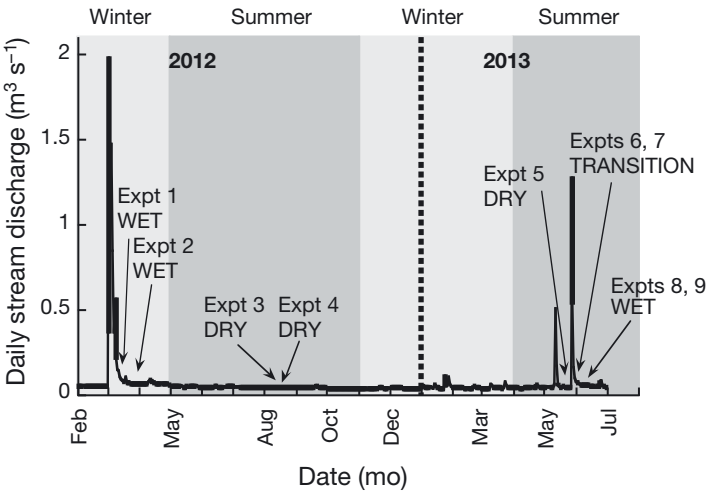

Fig. 2. Daily stream discharge from He'eia Stream over the course of our experiments (location of input to Kāne'ohe Bay indicated on Fig. 1). The x-axis covers the time period of all experiments from March 2012 through August 2013, and individual experiment times are noted on the figure, as are the season (winter or summer), year (2012 or 2013) and system state (wet, dry, transition). Data from the US Geological Survey National Water Information System (http://nwis.waterdata.usgs.gov/nwis/)

Microbial community abundances

Autotrophic community

The wet conditions of Expts 1, 8 and 9 had the highest overall phytoplankton biomass (90–98 µg C l^{-1}), followed by Expt 2 (82 µg C l^{-1}). PRO was present only in Expts 1 and 2. Under wet conditions, SYN increased in abundance, but larger (>3 µm) phytoplankton, including chain-forming *Chaeto-*

Table 1. Experiment sampling dates, environmental conditions (photosynthetically active radiation [PAR], wind direction and speed, rainfall, surface temperature [*T*], system state) and chl *a* at the beginning of each experiment in southern Kāneʻohe Bay. PAR is measured at the sea surface; wind direction and speed refer to averages (±SD) near the study site; rainfall is the total amount measured during the 2 wk prior to the sampling date. System states are defined as dry = background stream flow (<0.05 $m^3 s^{-1}$, Heʻeia Stream gauge) into the bay for 1 to 2 wk prior to sampling and wet = rain-induced increased stream flow (>1 $m^3 s^{-1}$, Heʻeia Stream gauge), bringing sediments and nutrients into the bay, 1 to 2 wk prior to and/or during sampling

Expt	Date	PAR surface (µmol $m^{-2} s^{-1}$)	Wind direction	Wind speed (knots)	Rainfall (mm)	*T* (°C)	System state	Chl *a* (µg l^{-1})
1	16 Mar 2012	1201	NE	13.5 ± 1.0	389	22	Wet	1.15
2	30 Mar 2012	1582	NNE	12.0 ± 2.7	14	23	Wet	0.71
3	5 Aug 2012	1735	ENE	10.5 ± 1.3	9	26	Dry	0.38
4	8 Aug 2012	1748	ENE	13.5 ± 1.0	13	26	Dry	0.52
5	27 May 2013	1454	NE	12.1 ± 1.1	6	26	Dry	0.37
6	29 May 2013	1490	ENE	7.9 ± 4.2	7	26	Transition	0.31
7	31 May 2013	1490	NE	9.8 ± 1.7	8	26	Transition	0.27
8	3 Jun 2013	1639	NE	12.8 ± 1.5	9	26	Wet	0.88
9	5 Jun 2013	1602	NE	12.2 ± 1.2	6	26	Wet	0.95

Table 2. Autotrophic microbial biomass (µg C l^{-1}) in Expts 1 to 9, reported as average (±SD) values. Groups listed are *Prochlorococcus* (PRO), *Synechococcus* (SYN), autotrophic eukaryotes (A-EUK), diatoms and autotrophic dinoflagellates (A-DF). Methods for quantifying each group were flow cytometry (FCM, duplicates), epi-fluorescence microscopy (EPI-MICRO) and inverted microscopy of acid Lugol's preserved samples (LUGOLS-MICRO). Biomass is calculated for each group as described in the section 'Microbial abundance and biomass'. nd: no data available; –: not present; Trans: Transition

Method Group	System state:	1 Wet	2 Wet	3 Dry	4 Dry	5 Dry	6 Trans	7 Trans	8 Wet	9 Wet
FCM										
PRO		6.7 ± 0.1	7.7 ± 0.6	–	–	–	–	–	–	–
SYN		34.1 ± 1.4	51.2 ± 2.9	17.6 ± 0.5	26.6 ± 0.4	6.8 ± 0.1	35.5 ± 3.8	17.8 ± 1.1	46.1 ± 0.7	52.8 ± 0.5
A-EUK (2–3 µm)		43.5 ± 4.1	17.9 ± 2.8	13.7 ± 0.5	19.5 ± 1.2	23.1 ± 1.9	21.0 ± 2.1	11.5 ± 1.2	22.2 ± 0.9	30.2 ± 0.3
EPI-MICRO										
A-EUK (3–10 µm)		nd	3.7 ± 2.4	5.9 ± 2.8	5.6 ± 2.0	3.9 ± 2.1	6.5 ± 4.2	15.2 ± 9.2	18.2 ± 8.2	10.6 ± 3.9
A-EUK (10–30 µm)		2.0 ± 2.4	1.1 ± 1.4	5.6 ± 1.9	3.8 ± 2.1	2.9 ± 2.0	1.2 ± 0.7	1.3 ± 1.6	2.1 ± 1.6	2.2 ± 2.1
LUGOLS-MICRO										
Diatoms		7.8 ± 6.9	0	0.9 ± 1.4	2.4 ± 2.8	0.04 ± 0.06	0	0	0.07 ± 0.09	0.4 ± 0.6
A-DF (>20 µm)		0.2	0.2	0.12	0.1	0	0.1	0.1	1.4	1.3
Total autotrophic + mixotrophic community		>94	82	44	58	33	64	46	90	98

ceros spp. centric diatoms, dominated biomass (Table 2). Larger (>20 µm) autotrophic dinoflagellates (A-DF) had 10-fold more biomass in Expts 8 and 9 wet conditions relative to the other experiments and were mainly represented by *Prorocentrum sigmoides* Böhm-like cells. Also present at low abundance in most experiments was the dinoflagellate *Akashiwo sanguinea* (Hirasaka) G. Hansen et Moestrup (Daugbjerg et al. 2000). Phytoplankton biomass was lower under dry or transition conditions (37–64 µg C l^{-1}). The dry condition phytoplankton communities were dominated by 2–3 µm A-EUK and SYN.

Heterotrophic community

The microzooplankton community (10–200 µm in length) included heterotrophic and mixotrophic protists and metazoan nauplii. Heterotrophic dinoflagellate (H-DF) and heterotrophic ciliate (H-CIL) biomass had a significant positive relationship with their nano- and microphytoplankton prey biomass (Fig. 3, $r^2 = 0.92$, *t*-test, $p < 0.05$). Larger (>20 µm) H-DF were mainly *Gyrodinium*, *Protoperidinium* or *Amphidinium* spp., and their highest biomass was found in wet conditions. H-CIL were mainly >20 µm aloricate oligotrichs. Mixotrophic ciliate

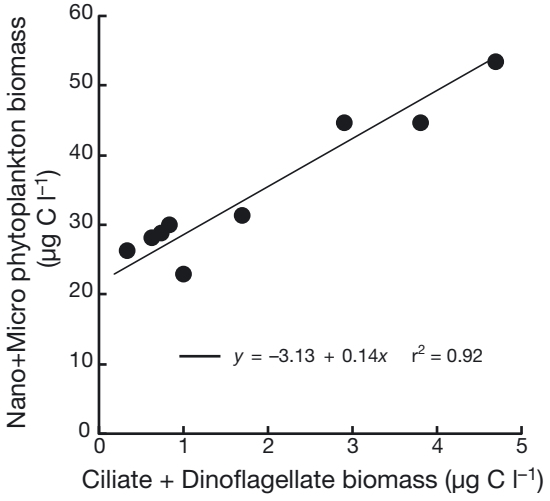

Fig. 3. Phytoplankton (nano- + microplankton) biomass as a function of microzooplankton (ciliate + dinoflagellate) biomass. Picophytoplankton biomass is not included, assuming that they are consumed by the smaller (nanoflagellate) microzooplankton. Linear regression shown on the figure

(M-CIL) species were *Mesodinium rubrum* Lohmann (1908), *Tontonia* sp. and *Laboea strobila* Lohmann (1908). Metazoan larvae had the highest biomass in the wet spring conditions of Expt 1 and, despite a dominance by copepod nauplii, also included polychaete and gastropod larvae (Table 3). In the other experiments, the lower metazoan biomass mainly comprised copepod nauplii.

Phytoplankton growth and mortality rates

Chl *a*-based rate measurements

Phytoplankton community growth and mortality rates, based on chl *a*, were available for Expts 3 to 9 (Table 4). The net growth response to dilution was invariably linear (Fig. 4), and except for Expt 4, all mortality rates were significantly different from zero (*t*-test, $p < 0.05$, Table 4). Growth rates were adjusted for photoadaptation (Table 4), with only Expt 6 showing a significant difference in growth rate (i.e. no correction: $\mu_0 = -0.21$ d^{-1}, with correction: $\mu_0 = 0.41$ d^{-1}). Phytoplankton responded to macronutrient additions in all cases, i.e. 0.2 d^{-1} in Expt 3 and ≥0.6 d^{-1} in all other experiments (Table 4). Microzooplankton-induced mortality (m) of the phytoplankton community was substantial, ranging from 0.3 to 0.7 d^{-1}, and accounted for over 100% of daily growth (m:μ_0, Table 4, negative μ_0 values set to 0.01 d^{-1}). Coefficients of determination (r^2), based on regressions of net growth rate as a function of dilution factor (proxy for grazing impact), were high ($r^2 \geq 0.7$) for 5 of 7 experiments.

Table 3. Heterotrophic biomass (µg C l^{-1}) in Expts 1 to 9, reported as average (±SD) values. Groups listed are heterotrophic bacteria, eukaryotes, ciliates, dinoflagellates and metazoan nauplii (H-BACT, H-EUK, H-CIL, H-DF and H-META, respectively), as well as mixotrophic ciliates (M-CIL). H-CIL are mainly *Strombidium* and *Strobilidium*, with occasional tintinnids. H-DF are mainly gymnodinids (e.g. *Gyrodinium*) and *Protoperidinium* spp. M-CIL are *Tontonia*, *Laboea strobila* and *Mesodinium rubrum.* H-META are mostly copepod nauplii and copepodites, but occasionally meroplanktonic larvae were present. Methods for quantifying each group were flow cytometry (FCM), epi-fluorescence microscopy (EPI-MICRO) and inverted microscopy of acid Lugol's preserved samples (LUGOLS-MICRO). nd: no data available; Trans: Transition

Method		1	2	3	4	5	6	7	8	9
Group	System state:	Wet	Wet	Dry	Dry	Dry	Trans	Trans	Wet	Wet
FCM										
H-BACT		14.3 ± 0.9	15.2 ± 0.7	7.6 ± 0.4	7.0 ± 0.2	3.5 ± 0.5	3.7 ± 0.1	6.3 ± 0.4	10.1 ± 0.3	11.2 ± 0.3
EPI-MICRO										
H-EUK (3–10 µm)		nd	20.0 ± 10.3	10.4 ± 3.0	8.4 ± 3.2	8.2 ± 3.2	10.4 ± 2.0	10.8 ± 5.8	11.9 ± 3.4	21.2 ± 13.7
H-EUK (10–20 µm)		9.5 ± 6.9	6.6 ± 3.5	7.5 ± 2.9	14.3 ± 10.0	5.5 ± 2.8	7.0 ± 4.6	5.8 ± 3.8	12.7 ± 4.8	27.5 ± 9.1
LUGOLS-MICRO										
H-CIL (<30 µm)		0.3	0.3	0.1	0.2	0.2	0.4	0.2	0.6	0.5
H-CIL (>30 µm)		1.2	0.1	0.02	0.1	0.1	0.01	0.03	0.4	0.7
H-DF (20–30 µm)		0.5	0.1	0.02	0	0.04	0.03	0.2	0.3	0.6
H-DF (>30 µm)		2.7	0.5	0.2	1.4	0.5	0.3	0.2	2.5	1.1
M-CIL		2.4	0.1	0.1	0.1	0.02	0	0.01	0.3	0.5
H-META		13 ± 6	1 ± 1	4 ± 2	2 ± 1	8 ± 3	8 ± 2	0.3 ± 0.2	2 ± 2	4 ± 3
Total heterotrophic community		>44	44	30	34	26	30	24	41	67

Table 4. Phytoplankton growth and mortality rates based on changes in chl *a* during 24 h seawater dilution incubation experiments. Shown are initial chl *a* concentrations, phytoplankton growth rates without added nutrients (μ_0) and with added nutrients (μ_N), mortality rates (*m*) and the coefficient of determination (r^2) for each reduced major axis regression. The only non-significant regression (*t*-test, $p \leq 0.05$) is for Expt 4 and is in *italics*. All rate data are adjusted for pigment photoadaptation during the incubation, using the weighted average *Synechococcus* and autotrophic eukaryote red fluorescence from parallel flow cytometry samples. The magnitude of the correction factor (CF) is shown. **Bold**: negative growth rates

Expt	Chl *a* (µg l^{-1})	μ_0 (d^{-1})	μ_N (d^{-1})	*m* (d^{-1})	r^2	CF (d^{-1})
3	0.38	**–0.03**	0.15	0.31	0.69	–0.01
4	0.52	**–1.01**	0.53	0.11	*0.01*	0.18
5	0.37	**–0.15**	0.47	0.74	0.86	–0.08
6	0.31	0.41	1.19	0.68	0.95	0.46
7	0.27	**–0.06**	0.99	0.47	0.26	0.03
8	0.88	**–0.68**	0.70	0.65	0.78	0.32
9	0.95	**–0.34**	0.71	0.45	0.94	0.22

Cell-based rate measurements

Under wet spring conditions, PRO were growing very fast (Expt 1, 1.56 d^{-1}), with a slight decrease in growth with macronutrient addition, and 79% of growth was lost to mortality (Table 5, Fig. 5). Two weeks later, PRO were growing more slowly (Expt 2, μ_0 = 0.61 d^{-1}) and were consumed at a higher rate than produced (*m*:μ_0 = 1.77), but growth increased ~36% with nutrient additions.

SYN showed positive growth rates in all experiments (1.14 ± 0.40 d^{-1}), with mortality rates averaging 0.58 ± 0.40 d^{-1} (Table 5, Fig. 5). The highest proportion of SYN biomass was consumed during wet periods (90%) and then transition periods (42%), with the lowest consumed during dry periods (27%).

Growth rates of H-BACT always exceeded 1 doubling per day (1.52 ± 0.42 d^{-1}, Table 5, Fig. 5), and ~3/4 of their growth was consumed daily. Their response to added inorganic nutrients was modest in 5 of 9 experiments (0.02 to 0.26 d^{-1}).

During wet conditions in Expt 1, 2–3 µm A-EUK growth was 1.50 d^{-1}, and no growth increase was seen with added nutrients; however, in Expt 2, 2 wk later, A-EUK growth was significantly slower (0.51 d^{-1}), and growth rates doubled with nutrient amendment (1.02 d^{-1}) (Table 5, Fig. 5). A-EUK growth rates were negative (–1.19 to –0.19 d^{-1}) in all other experiments. The effect of adding nutrients to Expts 3 to 9 varied, with some showing increased rates, some showing decreased rates and one showing no change (Expt 9). A-EUK mortality rates were 69 and 100% of growth in the wet conditions of Expts 1 and 2, respectively (Table 5). A-EUK in Expts 3, 5 and 6 experienced high mortality rates, while A-EUK in Expts 4, 8 and 9 had non-significant mortality rates (*m* = 0). Expt 7 A-EUK had negative mortality rates (–0.44 d^{-1}), which indicates that the dilution experiment assumptions were violated.

Microzooplankton growth and mortality rates

Growth rates of smaller (<30 µm) H-CIL were positive in 3 experiments (Expts 1, 3 and 7), with an average of 0.35 ± 0.13 d^{-1} (Table 6). They exhibited near-

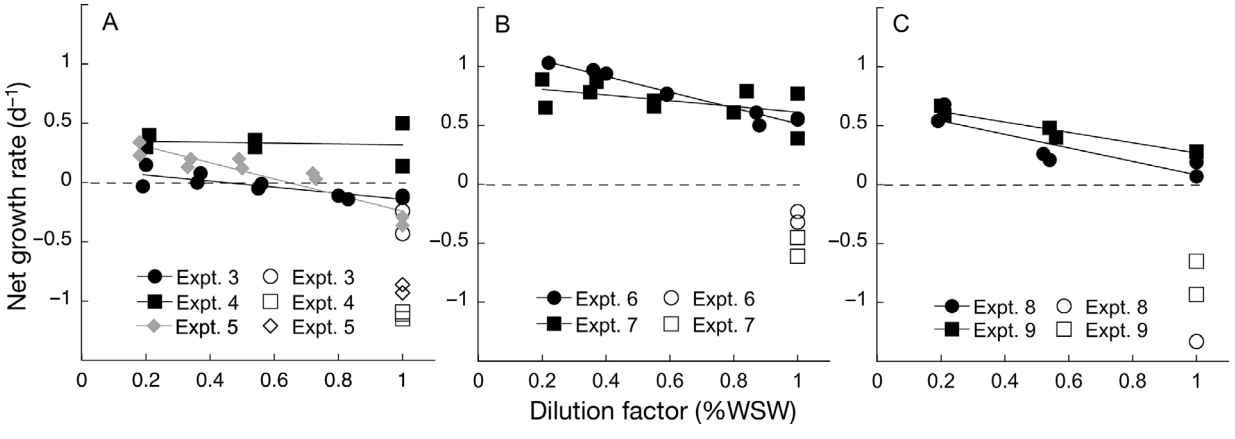

Fig. 4. Net phytoplankton growth rates for the entire phytoplankton community as a function of the whole seawater dilution factor (as percent whole seawater, % WSW), as measured by chl *a*. Shown are treatments with (filled symbols) and without (open symbols) added macronutrients (nitrogen and phosphorus). Reduced major axis regression results are reported in Table 4. (A) Dry condition Expts 3, 4 and 5; (B) transition condition Expts 6 and 7; (C) wet condition Expts 8 and 9

Table 5. Microbial growth and grazing rates in Expts 1 to 9. Shown are daily rate determinations for population-specific groups (as determined by flow cytometry) of *Prochlorococcus* (PRO), *Synechococcus* (SYN), autotrophic eukaryotes (A-EUK) and non-pigmented heterotrophic bacteria (H-BACT). Rates (d^{-1}) were determined with seawater dilution experiments and are reported as growth with no nutrient amendments (μ_0), growth with macronutrient amendments (μ_N) and mortality (m). Also shown is the coefficient of determination (r^2) for the reduced major axis regression of net growth rate as a function of dilution factor. Non-significant regressions are in *italics*. –: not present. **Bold**: negative growth rates

Expt	PRO				SYN				A-EUK				H-BACT			
	μ_0	μ_N	m	r^2	μ_0	μ_N	m	r^2	μ_0	μ_N	m	r^2	μ_0	μ_N	m	r^2
1	1.56	1.40	1.23	0.90	1.65	1.38	1.22	0.80	1.50	1.35	1.04	0.69	1.32	1.02	0.90	0.69
2	0.61	0.83	1.08	0.64	0.59	0.72	0.88	0.68	0.51	1.02	0.55	0.42	1.18	1.16	1.27	0.41
3	–	–	–	–	0.94	0.67	0.17	0.27	**–0.33**	**–0.43**	0.79	0.81	1.36	1.32	0.86	0.95
4	–	–	–	–	0.83	1.11	0.32	0.62	**–0.72**	**–0.36**	0.66	*0.22*	1.36	1.57	0.90	0.83
5	–	–	–	–	1.54	1.19	0.36	0.61	**–0.84**	**–0.35**	0.88	0.47	2.49	2.30	1.14	0.91
6	–	–	–	–	1.75	1.29	0.60	0.95	**–0.14**	**–0.33**	0.39	0.80	1.93	1.95	1.31	0.97
7	–	–	–	–	1.00	1.16	0.49	0.40	**–1.19**	**–0.13**	**–0.44**	0.25	1.41	1.60	1.06	0.82
8	–	–	–	–	0.97	1.29	0.79	0.86	**–0.19**	**–0.25**	0.35	*0.05*	1.25	1.51	1.04	0.89
9	–	–	–	–	0.99	1.38	0.54	0.87	**–0.20**	**–0.20**	0.17	*0.06*	1.41	1.64	1.07	0.94

zero or negative growth rates in the remaining experiments. This size class of H-CIL tended to experience high mortality rates during dry conditions (0.9–1.1 d^{-1}, 3 experiments) or, conversely, no mortality in most wet condition experiments (Expts 2, 8 and 9). The exception is Expt 1, where the mortality rate was high (1.42 d^{-1}) under wet conditions.

In Expts 1 and 9 (wet conditions), larger (>30 µm) H-CIL showed negative growth rates and low mortality rates but high biomass (Table 6). The lowest biomass of large H-CIL was in the transition Expt 6, which corresponded to zero growth and mortality rates. In the remaining 6 experiments, positive growth rates were found, along with mortality rates ranging from 0.11 to 4.29 d^{-1} (Table 6).

Smaller (20–30 µm) H-DF had positive growth in most experiments, with the exception of Expt 4 (smaller dinoflagellates absent) and Expt 8 (μ_Z = –2.42 d^{-1}) (Table 6). Mortality rates ranged from 0 (Expt 8) to 4.17 d^{-1} (Expt 9). Larger (>30 µm) H-DF had negative growth in 3 of 9 experiments (Expts 1, 2 and 4), zero growth in Expt 7 and positive growth (0.06–0.84 d^{-1}) in the remaining 5 experiments. Mortality rates were zero for the larger H-DF in 5 of 9 experiments but high in the rest of the experiments, which had significant biomass of metazoan nauplii in the incubation bottles.

DISCUSSION

Environmental context

Oligotrophic conditions in Kāne'ohe Bay during dry periods (Ringuet & Mackenzie 2005, Drupp et al. 2011) and otherwise favorable conditions for growth (sufficient irradiance, high temperature) suggest that the eukaryotic phytoplankton community was poised to take advantage of nutrient additions, as illustrated by the observed rapid (within 24 h) and often dramatic response to macronutrient additions. Wind-induced mixing of surface runoff in the bay has been shown to decrease the period of elevated surface nutrients (DeCarlo et al. 2007), and the highly variable chl *a* and nitrate data (Drupp et al. 2011) indicate frequent small-scale mixing events. This result has been found in other systems (Pinckney et al. 1999, Örnólfsdóttir et al. 2004) and is consistent with weather-related disturbances maintaining prokaryotic microbial diversity (Yeo et al. 2013). Our results suggest that this also applies to the bay's eukaryotic microbial community.

Phytoplankton community

SYN is the dominant cyanobacteria taxon in the bay and contributes ≥35% of phytoplankton biomass. SYN had positive net growth in 8 of the 9 experiments reported here, and in these experiments, microzooplankton grazing impact was 47 ± 22% (m:µ). Landry et al. (1984) reported a lower m:µ ratio (7–27%) for SYN, and Ayukai (1996) also found much higher SYN growth relative to mortality in a similar nitrogen-limited oligotrophic 26 to 27°C system on the Great Barrier Reef, Australia. Thus, SYN growth often exceeds mortality in oligotrophic coastal ecosystems (including Kāne'ohe Bay). In contrast, PRO were only detected in Expts 1 and 2, which

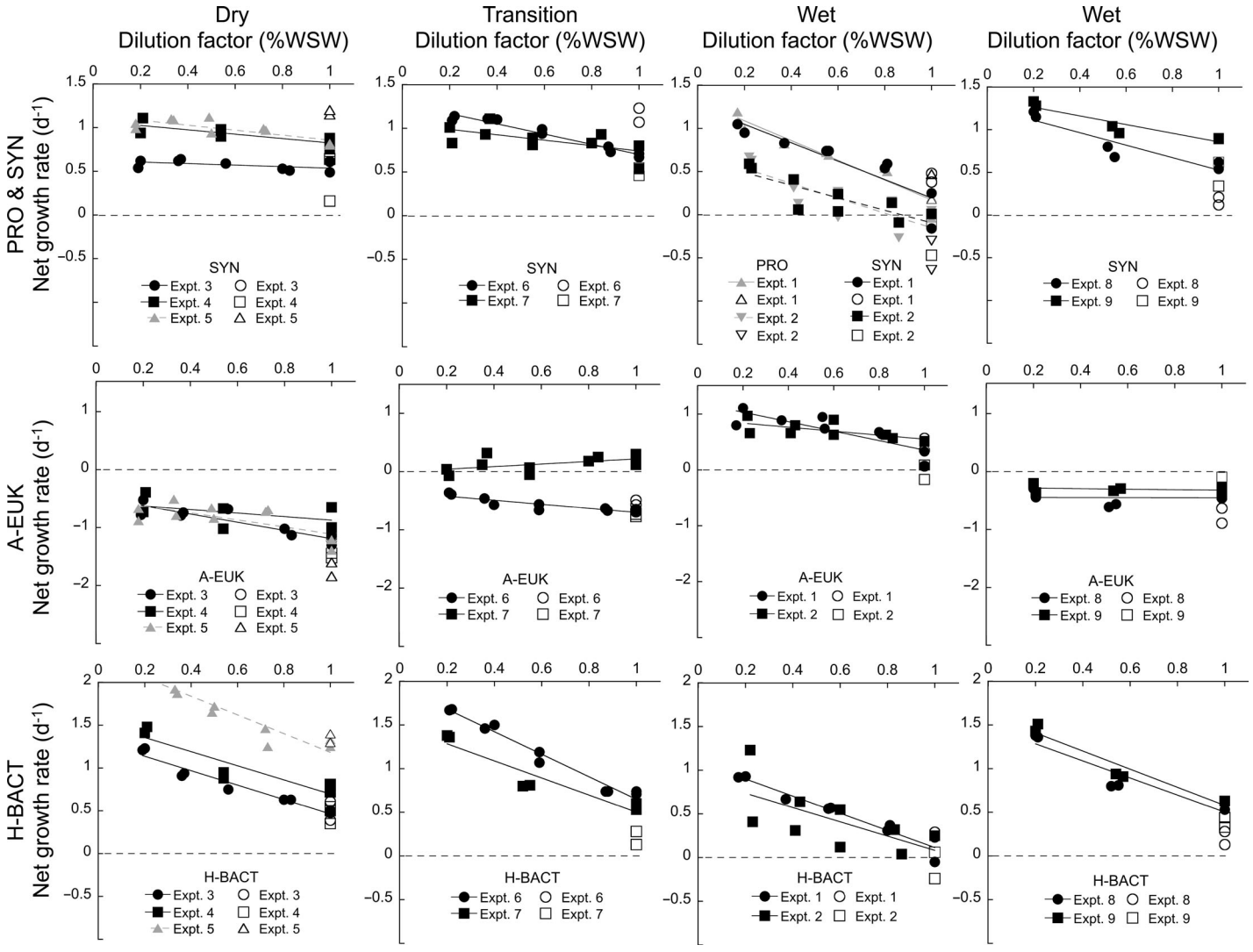

Fig. 5. Net cell-based growth rates for all phytoplankton populations as a function of dilution factor (percent whole seawater, % WSW), as measured by flow cytometry, and arranged by system state (left to right: dry, transition, wet). Populations are as follows: top row, *Prochlorococcus* (PRO, Expts 1 and 2 only) and *Synechococcus* (SYN); middle row, autotrophic eukaryotes (A-EUK); bottom row, heterotrophic bacteria (H-BACT). Experimental treatments with and without added macronutrients (nitrogen and phosphorus) are shown as filled and open symbols, respectively. Reduced major axis regression results are reported in Table 5 and are shown here as solid lines, except for Expts 2 and 5, where they are dashed lines for clarity. Symbol shapes represent each experiment (e.g. Expt 3 symbols are circles for all populations), with the exception of PRO in Expts 1 and 2, which are indicated by triangles. A horizontal dashed line in each panel is positioned at zero net growth rate

were subsequent to an extremely large storm event lasting several days, ending a dry period and causing the base flow of He'eia Stream to increase from ~0.08 to 2 $m^3 s^{-1}$. Along with this storm, the prevailing wind direction changed from normal NE trade winds to more northerly winds; the combined effect of variable winds and high stream flow likely caused more exchange of the bay water with offshore water and temporarily decreased seawater residence time within the southern bay. This advective transport is the likely source of PRO in the southern bay, as this taxon usually only occurs in the extremely oligotrophic waters outside the bay and sometimes in the most northerly portion of the bay (Monger & Landry 1993, Liu et al. 1995, Cox et al. 2006). Both PRO and SYN were growing at essentially the same rate in Expts 1 and 2, and in Expt 1, they were both being consumed at similar rates. However, PRO was consumed faster than SYN in Expt 2—indicating that PRO might be preferred prey and possibly explaining its usual absence in the bay, as has been hypothesized by Worden et al. (2004).

Table 6. Heterotrophic ciliate and dinoflagellate initial biomass (Z_0, µg C l^{-1}), estimated growth (μ_Z, d^{-1}) and mortality (m_Z, d^{-1}) rates in Expts 1 to 9. Cells are divided into <30 and ≥30 µm length categories. Mixotrophic species are not included in the biomass and rate estimates. **Bold**: negative growth rates

Expt	Ciliates						Dinoflagellates					
	<30 µm length			>30 µm length			20–30 µm length			>30 µm length		
	Z_0	μ_Z	m_Z	Z_0	μ_Z	m_Z	Z_0	μ_Z	m_Z	Z_0	μ_Z	m_Z
1	0.29	0.30	1.42	1.20	**−0.95**	0.10	0.47	1.42	2.37	2.72	**−0.72**	0.69
2	0.26	0.04	0	0.06	2.27	0.11	0.07	1.25	0.36	0.50	**−0.17**	0
3	0.12	0.50	1.17	0.02	0.28	0.28	0.02	1.38	0.11	0.18	0.58	1.72
4	0.20	**−0.34**	0.96	0.12	0.45	0.45	0	0	0	1.42	**−0.10**	0
5	0.22	**−0.57**	0.93	0.12	0.86	4.29	0.04	0.95	1.05	0.52	0.10	0.50
6	0.40	**−1.61**	0	0.01	0	0	0.03	0.18	0.91	0.27	0.06	0.29
7	0.18	0.25	1.05	0.03	0.62	0	0.15	0.47	1.04	0.17	0	0
8	0.56	**−2.24**	0	0.42	1.10	2.36	0.27	**−2.42**	0	2.48	0.33	0
9	0.54	**−1.23**	0	0.73	**−0.22**	0	0.56	0.83	4.17	1.06	0.84	0

Autotrophic eukaryote growth rates were highest in the high flow condition experiments, with positive growth in Expts 1 and 2, and although they had negative growth in the other experiments, the least negative growth rates were observed in Expts 8 and 9 (Table 5). Negative growth rates for naturally occurring eukaryotic phytoplankton have been reported (Kagami & Urabe 2001, Liu et al. 2002, Bec et al. 2005, Berninger & Wickham 2005, Collos et al. 2005, First et al. 2007, Calbet et al. 2011) and are usually attributed to viral lysis or artifacts of the seawater dilution technique. Since the prokaryotic autotrophic and heterotrophic populations showed reasonable growth rates, and the autotrophic eukaryotes had positive growth in some experiments, there is no evidence to suggest failure of the dilution experiment.

Dolan & McKeon (2005) raised concerns that microzooplankton grazing as measured by the seawater dilution method is overestimated, particularly in oligotrophic regions, based on the argument that unrealistically high ciliate clearance rates (>20 µl ciliate^{-1} h^{-1}) are inferred from the experimentally determined mortality rate. The average mortality rate from these experiments (chl *a*) was 0.49 ± 0.22 d^{-1}. However, reasonable clearance rates are found for the experiments reported here (3–25 µl ciliate^{-1} h^{-1}, Table 7), based on the chl *a*-based phytoplankton mortality rates from individual experiments (Table 4). If dinoflagellate and smaller flagellate consumers are considered, these ciliate clearance rates would be even lower. Thus, the data reported here are considered a reasonable assessment of microzooplankton impacts on phytoplankton.

Autotrophic eukaryote mortality rates due to grazing were high (0.6 ± 0.2 d^{-1}) in all experiments except Expt 7, where the A-EUK may have been starved for nutrients and thus of substandard nutritional quality for micrograzers (Table 5). Ciliates, which use chemoreception for prey selection (Verity 1988, 1991, Gonzalez et al. 1990), often actively avoid stationary phase phytoplankton and preferentially consume fast-growing species (Verity 1988), whereas the Expt 7 A-EUK were dying at a fast rate (μ_0 = −1.19 d^{-1}) and showed the most dramatic increase in growth with macronutrient additions relative to any other experiment (Fig. 5).

Table 7. Heterotrophic ciliate initial abundance in each experiment, along with estimated clearance rates, assuming that the majority of mortality estimated from chl *a*-based dilution experiments (*m* [d^{-1}], Table 4) is due to ciliates. Abundance data are from settled acid Lugol's preserved samples, using inverted microscopy. Ciliates are grouped into size categories, based on their longest length measurement. Clearance rates = ciliate abundance × *m*. nd: no data available

Expt	<10 µm (cells l^{-1})	10–20 µm (cells l^{-1})	20–30 µm (cells l^{-1})	>30 µm (cells l^{-1})	Total (cells l^{-1})	Clearance rate (µl ciliate^{-1} h^{-1})
1	929	714	179	3036	4857	nd
2	71	857	321	179	1429	nd
3	143	464	36	107	750	17
4	893	750	250	107	2000	3
5	321	821	214	0	1357	23
6	357	1214	393	0	1964	14
7	107	571	71	36	786	25
8	429	964	500	571	2464	11
9	107	607	429	464	1607	12

Comparable studies

The most comparable study for phytoplankton growth and mortality rates is that of Landry et al. (1984), conducted in Kāneʻohe Bay during September 1982, which reported an ambient concentration of 0.48 µg chl *a* l^{-1}. They found that 47% of the autotroph biomass was dominated by *Chlorella* sp., with few diatoms. This state of the bay is most comparable to our dry conditions, with ~0.4 to 0.5 µg chl *a* l^{-1}; however, no dominant eukaryotic phytoplankton group was evident. Other southern bay studies include Ringuet & Mackenzie (2005), who found baseline conditions (2001–2003) of 0.50 ± 0.28 µg chl *a* l^{-1}, and the 2.5 yr study of Drupp et al. (2011), who reported a summer average of 0.48 ± 0.28 µg chl *a* l^{-1} (December 2005–June 2008).

Landry et al. (1984) estimated a total community carbon of 86 µg C l^{-1}, with 65 µg C l^{-1} represented by phytoplankton. Our phytoplankton biomass estimates for Expts 3 and 4 are 44 and 58 µg C l^{-1}, respectively, which is remarkably similar, given the different approaches for estimating biomass. In contrast, heterotrophic consumer biomass (i.e. not including heterotrophic bacteria) in these experiments was ~24 µg C l^{-1}, relative to Landry et al.'s (1984) estimate of ~13 µg C l^{-1}. Thus, the ratio of heterotroph:autotroph biomass for Expts 3 and 4 (~24/58 = 0.41) is twice as high in the present study relative to the 1982 study (~13/65 = 0.20), which suggests a greater role of microzooplankton in controlling phytoplankton populations and a higher turnover rate of the community.

Assuming the same community is sampled over time, given the relatively long residence time of water in the southern part of Kāneʻohe Bay (Smith et al. 1981), the data from Expts 5 to 9 show evidence for a lag in phytoplankton community response to environmental forcing—taking at least 4 d to show a chl *a* increase after elevated stream discharge into the bay (28 May event, Table 1), with this effect persisting for at least 8 d (i.e. elevated chl *a* continues to Expt 9). This time frame is similar to the lag of ~5 d observed in Hoover et al. (2006) for increased chl *a* after a storm event and is within the 3–7 d response observed by Cox et al. (2006). Also, similar to Hoover et al. (2006), smaller (3–10 µm) autotrophic eukaryotes showed the most rapid increase after the stream input event (Table 2), from ~4 to 6.5 µg C l^{-1} in 2 d (Expts 5 and 6) and then to 15 µg C l^{-1} at 4 d (Expt 7). Hoover et al. (2006) also observed a peridinin peak (autotrophic dinoflagellates) at 3 d post-storm, followed by a fucoxanthin peak (diatoms) at 5 d post-storm. This general trend was also seen during Expts 5 to 9, since >20 µm autotrophic dinoflagellates increased 10-fold in biomass from Expts 5 to 8 (mainly comprising *Prorocentrum sigmoides* Böhm-like cells), while diatoms only doubled during that period but then increased 10-fold by Expt 9. Heterotrophic biomass also increased, reaching a high biomass by Expt 8, with most populations still increasing to Expt 9 (Table 3). Also, like in Hoover et al. (2006), elevated concentrations of the heterotrophic dinoflagellate *Protoperidinium* spp., a known diatom consumer, were observed in Expts 8 and 9, 6 d after the stream discharge event.

Microzooplankton community

Similar to the autotrophic community, the ciliate and dinoflagellate communities were distinctly different in the high stream flow vs. dry condition experiments. In Expt 1, oligotrich ciliates dominated, with ~45 to 60% of them mixotrophic taxa. Mixotrophic ciliates do not compete with phytoplankton for inorganic nitrogen but are limited by suitable prey for phagocytosis (Stoecker et al. 1988). Thus, their dominance in Kāneʻohe Bay under wet conditions suggests that they may be prey limited under the dry ecosystem state (lower prey biomass, Table 2). Mixotrophic ciliates also remineralize ammonia at the same rates as non-mixotrophic ciliates, obtaining this nutrition from phagocytized prey, so are considered a source, rather than a sink, of reduced nitrogen (Dolan 1997). The large (>30 µm) mixotrophic ciliate species *Laboea strobila* and *Tontonia* sp. may be particularly important in transferring primary production to higher trophic levels as direct food sources for naupliar copepods, meroplankton larvae and the relatively small-bodied adult copepod species found in Kāneʻohe Bay (Jungbluth & Lenz 2013).

The smaller (<30 µm) heterotrophic ciliates had much slower growth (0.3 ± 0.2 d^{-1}) than larger cells (0.8 ± 0.7 d^{-1}; note that neither average includes the negative rate estimates), as was found in the northern coastal Gulf of Alaska (Strom et al. 2007). Montagnes (1996) showed that cultures of *Strobilidium* and *Strombidium* spp. rapidly die (negative growth rates) if suitable prey biomass is too low. The negative growth rates found here tended to be associated with higher standing stocks of ciliates and suggest that heterotrophic ciliates were usually prey limited and in a highly variable environment, with daily changes occurring in community dynamics.

The greatest biomass contributions to total heterotrophic eukaryote biomass came from <20 µm consumers. Smaller (20–30 µm) dinoflagellates generally showed higher growth rates than larger (>30 µm) forms, as reported by Hansen (1992). The average growth rate for the smaller heterotrophic dinoflagellates (without the single highly negative rate in Expt 8) was 0.9 ± 0.5 d^{-1}, whereas it was 0.3 ± 0.3 d^{-1} for the larger forms (the latter average does not include the 3 negative rates), which is in the range of maximum growth rates reported elsewhere (Jakobsen & Hansen 1997, Anderson & Menden-Deuer 2017). This is opposite to the pattern found for the 2 heterotrophic ciliate size groups, suggesting that the ciliates were more prey limited than the dinoflagellates. The negative growth rate (–0.72 d^{-1}) observed for the >30 µm heterotrophic dinoflagellates in Expt 1 may represent the community adjusting to the end of the diatom bloom and going into a starvation mode (Hansen 1992, Menden-Deuer et al. 2005). By Expt 2, conducted 2 wk later, the >30 µm heterotrophic dinoflagellate biomass was 5 times lower. Similarly, in Expt 4, the >30 µm heterotrophic dinoflagellate biomass was much higher than in Expt 3 (1.42 vs. 0.18 µg C l^{-1}, respectively), but growth decreased over the 3 d interval between experiments from 0.58 to –0.10 d^{-1}, suggesting adjustment towards a starvation survival mode.

Complex food web interactions

A proposed lower trophic level food web for the southern part of Kāneʻohe Bay is shown in Fig. 6, with an emphasis on identifying pathways of trophic transfer from microbial to metazoan consumers. During dry (low stream flow) conditions, the phytoplankton community (trophic level 1 [TL1]) was dominated by SYN and smaller (2–10 µm) autotrophic eukaryotes, with small (3–10 µm) heterotrophic eukaryotes (H-EUK) as the primary consumers (trophic level 2 [TL2], Table 7). H-BACT are not included in the diagram but also are prey for H-EUK. At trophic level 3 (TL3), 10–30 µm ciliates (H-CIL) mainly consume smaller A-EUK and H-EUK. H-DF prefer prey closer to their own size (Hansen et al. 1994, Jeong et al. 2010) and therefore are members at TL3 to trophic level 4 (TL4). Finally, metazoan nauplii and larvae (copepods and meroplankton) consume TL3 H-CIL and TL3 or TL4 H-DF, in addition to smaller cells (Vogt et al. 2013, Saiz et al. 2014, Jungbluth et al. 2017), and they may be feeding across TL2 to trophic level 5 (TL5). Related studies on naupliar grazing conducted concurrently with Expts 5 to 9 found changing naupliar prey preference across the 10 d period 27 May to 5 June 2013 (Jungbluth et al. 2017). Under dry, background ecosystem states with lower total biomass in the community (Expts 5 and 6), Jungbluth et al. (2017) showed that calanoid nauplii were feeding significantly on readily available smaller cells.

Under wet (high stream flow) conditions, with an increase in macronutrient inputs, including silicic acid, diatoms were episodically important (Fig. 6). PRO, along with heterotrophic bacteria and SYN, served as prey for the smaller 3–10 µm nano-H-EUK (TL2). Under these conditions, larger autotrophic dinoflagellates were also present, as well as very large (>30 µm) heterotrophic dinoflagellates and ciliates. The larger H-CIL were likely feeding directly on the larger phytoplankton (TL2), while the >30 µm heterotrophic dinoflagellates were consuming ciliates, >30 µm heterotrophic dinoflagellates and the diatoms (TL3 and TL4). Under these conditions, many of the ciliates were mixotrophic (M-CIL) but obligate phagotrophs on mostly smaller A-EUK (TL2). Metazoans were present at elevated abundance (e.g. Expt 1, Table 3) and may have been feeding on any of the larger cells (TL2 to TL5). Concurrent naupliar grazing experiments found selective feeding on larger cells during periods of higher prey availability under high stream flow ecosystem conditions (i.e. *Bestiolina similis*, Jungbluth et al. 2017). Higher total biomass in the community under wet ecosystem conditions (Expts 1–2 and 8–9) represents greater prey availability for metazoans and increasing prevalence of efficiently captured larger cells (dinoflagellates, ciliates). This shift in metazoan grazing preference towards larger cells may account for the high ciliate and dinoflagellate mortality rates found in seawater dilution Expts 8 and 9 (Table 6).

Ciliates and dinoflagellates form a major trophic link between primary producers and higher TLs in Kāneʻohe Bay, despite significant metabolic losses during trophic transfer. Ciliates occupy TL3 or higher in Kāneʻohe Bay; thus, less than 10% of primary production would be expected to form their biomass (i.e. at 30–40% gross growth efficiency per step, ~9–16% of primary production would reach TL3). Lynn et al. (1991), working in a similar system in tropical waters off Kingston, Jamaica, also concluded that ~14% of primary production was funneled through ciliates to higher TLs. This inference, on the TL3 position of ciliates, is supported by the slope of 0.14 (Fig. 3), representing the autotrophic carbon comprising ciliates and dinoflagellates. Thus, in these picoplankton-

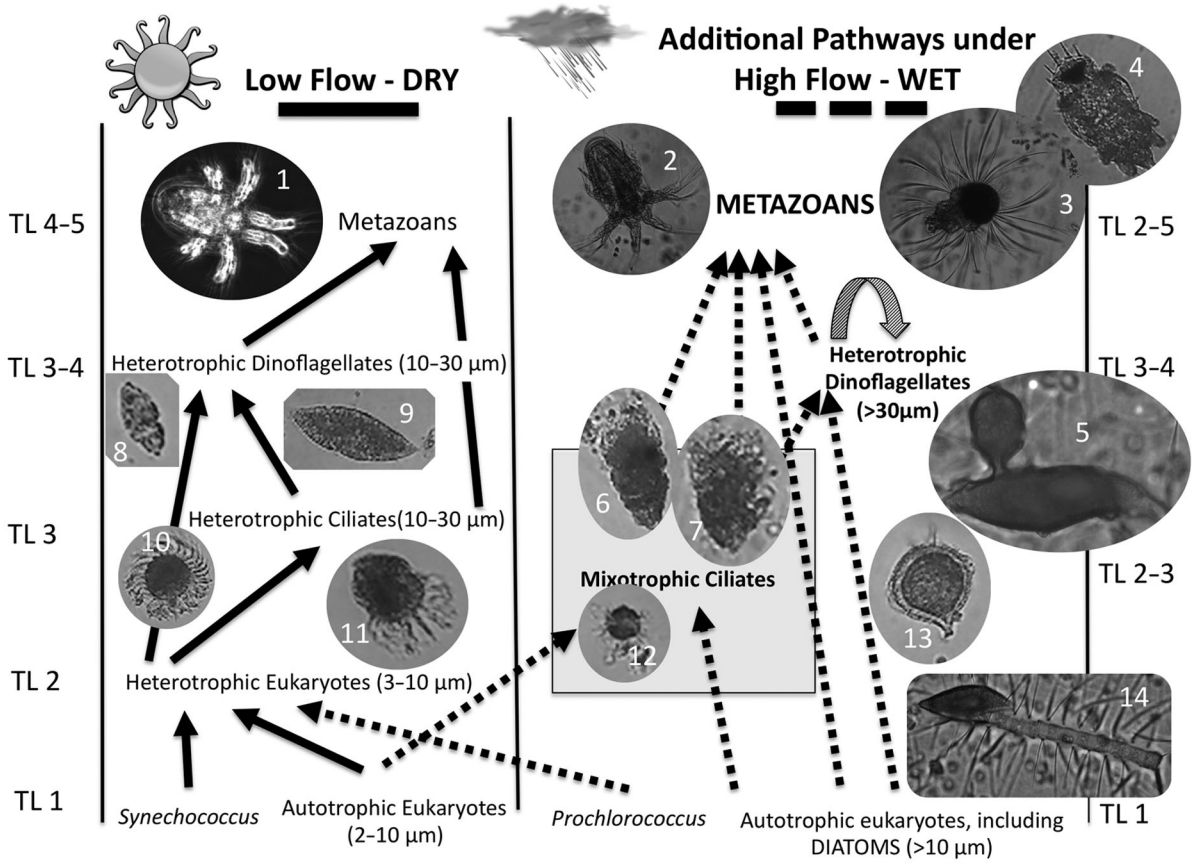

Fig. 6. Microbial food web in southern Kāne'ohe Bay under high and low stream flow ecosystem states, corresponding to dry and wet states, respectively. Thick solid lines (left side) show predator–prey relationships during low stream flow conditions, and thick dotted lines (right side) show additional trophic pathways that occur under high stream flow ecosystem states. Along the left and right are proposed trophic level (TL) 1 to TL 5, with TL 1 at the autotroph level and the highest microzooplankton consumer at TL 5 (metazoan nauplii and larval forms). Primary functional groups of organisms are shown at each trophic level. Autotrophs shown include *Synechococcus*, *Prochlorococcus*, autotrophic eukaryotes and diatoms. Consumers shown include heterotrophic eukaryotes (3–10 µm), dinoflagellates and ciliates, mixotrophic ciliates, and metazoan larvae and nauplii (including copepod and meroplankton species). The cloud and sun symbols indicate high and low stream flow ecosystem states. Numbered images refer to the following: 1, copepod nauplius; 2, copepod nauplius; 3, polychaete nauplius; 4, unknown meroplankton larva; 5, dinoflagellate consuming dinoflagellate via peduncle; 6, *Laboea strobila*; 7, *Tontonia* sp.; 8, *Gyrodinium* sp.; 9, *Gyrodinium* sp.; 10, aloricate ciliate; 11, aloricate ciliate; 12, *Mesodinium rubrum*; 13, *Protoperidinium* sp.; 14, diatom chain (*Chaetoceros* sp.) with *Gyrodinium* consumer

dominated ecosystems, a large fraction of primary production is too small to be efficiently captured directly by metazoan consumers, and microzooplankton are therefore the main primary production conduits to higher TLs.

CONCLUSIONS

As the dominant consumers of phytoplankton in all marine ecosystems, microzooplankton control the fate of primary production and the extent of carbon transfer to higher trophic level consumers (e.g. metazoans). Unlike temperate environments, where communities are driven by seasonal changes in temperature and photoperiod, we demonstrate that in an oligotrophic coastal embayment (Kāne'ohe Bay), ecosystem dynamics alternate between stable dry ecosystem states, with persistent macronutrient limitation of phytoplankton growth, to episodically storm-influenced wet ecosystem states, with distinct microbial food web community structure and dynamics (growth, mortality). *Synechococcus* and picoeukaryote (2–3 µm) biomass dominates the phytoplankton community under dry ecosystem states. *Prochlorococcus* can be found in the southern bay during wet ecosystem states but do not persist during dry periods. Rapid growth of *Synechococcus* is observed in both ecosystem states, but eukaryotic phytoplankton growth is negative under dry condi-

tions. Larger heterotrophic consumers, dinoflagellates *Gyrodinium and Protoperidinium* spp. and mixotrophic ciliates *Laboea strobila* and *Tontonia* sp. also appear in the ecosystem immediately following storms, augmenting the number of trophic pathways by which carbon moves from the microbial community to metazoan consumers. Trophic complexity of the ecosystem increases in post-storm wet states, and with higher total community biomass, the microbial food web supports higher transfer of production to metazoans, which often show a numerical response to storm inputs and altered recruitment in the post-storm period (e.g. Hoover et al. 2006, Jungbluth 2016, 2017). Our results provide some of the first observations on microzooplankton community dynamics from oligotrophic coastal ecosystems, including the relatively well studied Kāne'ohe Bay. Future work should focus on resolving whether autotrophic eukaryotes regularly have negative growth rates under dry conditions, as well as determining their responses to silicate addition, and assessing benthic contributions to nutrient enrichment, perhaps with the use of *in situ* dialysis incubation chambers. Another open question is the trophic role of the transient mixotrophic ciliate populations, including identifying their mortality agents.

Acknowledgements. We thank G. Batzel for assistance in the field and S. Chang and M. Uchida for assistance in microscopy and sample/image analysis. This is SOEST contribution no. 10276. This research was partially supported by University of Hawai'i Sea Grant program grant No. R/HE-18 and National Science Foundation grant OCE-1255697 to E.G., K.E.S. and P.H.L.

LITERATURE CITED

Almeda R, Calbet A, Alcaraz M, Saiz E and others (2011) Trophic role and carbon budget of metazoan microplankton in northwest Mediterranean coastal waters. Limnol Oceanogr 56:415–430

Anderson SR, Menden-Deuer S (2017) Growth, grazing and starvation survival in three heterotrophic dinoflagellates species. J Eukaryot Microbiol 64:213–225

Ayukai T (1996) Possible limitation of the dilution technique for estimating growth and grazing mortality rates of picoplanktonic cyanobacteria in oligotrophic tropical waters. J Exp Mar Biol Ecol 198:101–111

Bec B, Jusseini-Ratrema J, Collos Y, Souchu P, Vaquer A (2005) Phytoplankton seasonal dynamics in a Mediterranean coastal lagoon: emphasis on the picoeukaryote community. J Plankton Res 27:881–894

Berninger UG, Wickham SA (2005) Response of the microbial food web to manipulation of nutrients and grazers in the oligotrophic Gulf of Aqaba and northern Red Sea. Mar Biol 147:1017–1032

Bienfang PK, Takahashi M (1983) Ultraplankton growth rates in a subtropical ecosystem. Mar Biol 76:213–218

Bohonak AJ, van der Linde K (2004) RMA: software for reduced major axis regression, Java version. www.kimvdlinde.com/professional/rma.html

Böttjer D, Morales CE (2005) Microzooplankton grazing in a coastal embayment off Concepción, Chile, (~36° S) during non-upwelling conditions. J Plankton Res 27: 383–391

Buitenhuis WK, Li W, Vaulot D, Lomas MW and others (2012) Picophytoplankton biomass distribution in the global ocean. Earth Syst Sci Data 4:37–46

Calbet A, Landry M (1999) Mesozooplankton influences on the microbial food web: direct and indirect trophic interactions in the oligotrophic open ocean. Limnol Oceanogr 44:1370–1380

Calbet A, Landry M (2004) Phytoplankton growth, microzooplankton grazing, and carbon cycling in marine systems. Limnol Oceanogr 49:51–57

Calbet A, Landry MR, Scheinberg RD (2000) Copepod grazing in a subtropical bay: species-specific responses to a midsummer increase in nanoplankton standing stock. Mar Ecol Prog Ser 193:75–84

Calbet A, Saiz E, Almeda R, Movilla JI, Alcaraz M (2011) Low microzooplankton grazing rates in the Arctic Ocean during a *Phaeocystis pouchetii* bloom (summer 2007): fact or artifact of the dilution technique? J Plankton Res 33:687–701

Campbell L, Vaulot D (1993) Photosynthetic picoplankton community structure in the subtropical North Pacific Ocean near Hawai'i (station ALOHA). Deep Sea Res I 40: 2043–2060

Campbell L, Nolla HA, Vaulot D (1994) The importance of *Prochlorococcus* to community structure in the central North Pacific Ocean. Limnol Oceanogr 39:954–961

Chen B, Liu H, Landry MR, Chen M and others (2009) Estuarine nutrient loading affects phytoplankton growth and microzooplankton grazing at two contrasting sites in Hong Kong coastal waters. Mar Ecol Prog Ser 379:77–90

Christian JR, Karl DM (1994) Microbial community structure at the US-Joint Global Ocean Flux Study Station ALOHA: inverse methods for estimating biochemical indicator ratios. J Geophys Res 99:14269–14276

Collos Y, Husseini-Ratrema J, Bec B, Vaquer A and others (2005) Pheopigment dynamics, zooplankton grazing rates and the autumnal ammonium peak in a Mediterranean lagoon. Hydrobiology 550:83–93

Cox EF, Ribes M, Kinzie RA III (2006) Temporal and spatial scaling of planktonic responses to nutrient inputs into a subtropical embayment. Mar Ecol Prog Ser 324:19–35

Daugbjerg N, Hansen G, Larsen J, Moestrup Ø (2000) Phylogeny of some of the major genera of dinoflagellates based on ultrastructure and partial LSU rDNA sequence data, including the erection of three new genera of unarmoured dinoflagellates. Phycologia 39:302–317

De Carlo EH, Hoover DJ, Young CW, Hoover RS, Mackenzie FT (2007) Impact of storm runoff from tropical watersheds on coastal water quality and productivity. Appl Geochem 22:1777–1797

Dolan JR (1997) Phosphorus and ammonia excretion by planktonic protists. Mar Geol 139:109–122

Dolan JR, McKeon K (2005) The reliability of grazing rate estimates from dilution experiments: Have we overestimated rates of organic carbon consumption by microzooplankton? Ocean Sci 1:1–7

Drupp P, De Carlo EH, Mackenzie FT, Bienfang P, Sabine

CL (2011) Nutrient inputs, phytoplankton response, and CO_2 variations in a semi-enclosed subtropical embayment, Kāne'ohe Bay, Hawai'i. Aquat Geochem 17: 473–498

First MR, Lavrentyev PJ, Jochem FJ (2007) Patterns of microzooplankton growth in dilution experiments across a trophic gradient: implications for herbivory studies. Mar Biol 151:1929–1940

First MR, Miller HL III, Lavrentyev PJ, Pinckney JL, Burd AB (2009) Effects of microzooplankton growth and trophic interactions on herbivory in coastal and offshore environments. Aquat Microb Ecol 54:255–267

Furnas M (2007) Intra-seasonal and inter-annual variations in phytoplankton biomass, primary production and bacterial production at North West Cape, Western Australia: links to the 1997–1998 El Niño event. Cont Shelf Res 27: 958–980

Garrison DL, Gowing MM, Hughes MP, Campbell L and others (2000) Microbial food web structure in the Arabian Sea: a US JGOFS study. Deep Sea Res II 47: 1387–1422

Gonzalez JM, Sherr EB, Sherr BF (1990) Size-selective grazing on bacteria by natural assemblages of estuarine flagellates and ciliates. Appl Environ Microbiol 56:583–589

Hansen B, Bjornsen PK, Hansen PJ (1994) The size ratio between planktonic predators and their prey. Limnol Oceanogr 39:395–403

Hansen PJ (1992) Prey size selection, feeding rates and growth dynamics of heterotrophic dinoflagellates with special emphasis on *Gyrodinium spirale.* Mar Biol 114: 327–334

Hoover RS, Hoover D, Miller M, Landry MR, DeCarlo EH, Mackenzie FT (2006) Zooplankton response to storm runoff in a tropical estuary: bottom-up and top-down controls. Mar Ecol Prog Ser 318:187–201

Hopcroft RR, Roff JC (1990) Phytoplankton size fractions in a tropical neritic ecosystem near Kingston, Jamaica. J Plankton Res 12:1069–1088

Jakobsen HH, Hansen PJ (1997) Prey size selection, grazing and growth response of the small heterotrophic dinoflagellate *Gymnodinium* sp. and the ciliate *Balanion comatum*—a comparative study. Mar Ecol Prog Ser 158:75–86

Jeong, HJ, Du Yoo, Y, Kim, JS, Seong, KA, Kang, NS, Kim, TH (2010) Growth, feeding and ecological roles of the mixotrophic and heterotrophic dinoflagellates in marine planktonic food webs. Ocean Sci J 45:65–91

Jungbluth MJ (2016) Copepod nauplii and their roles in planktonic marine food webs. PhD dissertation, University of Hawai'i at Mānoa, Honolulu, HI

Jungbluth MJ, Lenz PH (2013) Copepod diversity in a subtropical bay based on a fragment of the mitochondrial COI gene. J Plankton Res 35:630–643

Jungbluth MJ, Selph KE, Lenz PH, Goetze E (2017) Species-specific grazing and significant trophic impacts by two species of copepod nauplii, *Parvocalanus crassirostris* and *Bestiolina similis*. Mar Ecol Prog Ser 572:57–76

Kagami M, Urabe J (2001) Phytoplankton growth rate as a function of cell size: an experimental test in Lake Biwa. Limnology 2:111–117

Kimmerer WJ (1984) Selective predation and its impact on prey of *Sagitta enflata* (Chaetognatha). Mar Ecol Prog Ser 15:55–62

Landry MR, Hassett RP (1982) Estimating the grazing impact of marine micro-zooplankton. Mar Biol 67: 283–288

Landry MR, Haas LW, Fagerness VL (1984) Dynamics of microbial plankton communities: experiments in Kāne'ohe Bay, Hawai'i. Mar Ecol Prog Ser 16:127–133

Liu H, Campbell L, Landry MR (1995) Growth and mortality rates of *Prochlorococcus* and *Synechococcus* measured with a selective inhibitor technique. Mar Ecol Prog Ser 116:277–287

Liu HB, Suzuki K, Saino T (2002) Phytoplankton growth and microzooplankton grazing in the subarctic Pacific Ocean and the Bering Sea during summer 1999. Deep Sea Res I 49:363–375

Lohmann H (1908) Beziehung zwischen biomasse und stickstoffgehalt des phytoplanktons. Schweiz Z Hydrol 31: 110–127

Lynn DH, Roff JC, Hopcroft RR (1991) Annual abundance and biomass of aloricate ciliates in tropical neritic waters off Kingston, Jamaica. Mar Biol 110:437–448

Menden-Deuer S, Lessard EJ (2000) Carbon to volume relationships for dinoflagellates, diatoms, and other protist plankton. Limnol Oceanogr 45:569–579

Menden-Deuer S, Lessard EJ, Satterberg J, Grünbaum D (2005) Growth rates and starvation survival of three species of the pallium-feeding, thecate dinoflagellate genus *Protoperidinium.* Aquat Microb Ecol 41:145–152

Monger BC, Landry MR (1993) Flow cytometric analysis of marine bacteria with Hoechst 33342. Appl Environ Microbiol 59:905–911

Montagnes DJS (1996) Growth responses of planktonic ciliates in the genera *Strobilidium* and *Strombidium.* Mar Ecol Prog Ser 130:241–254

Örnólfsdóttir EB, Lumsden SE, Pinckney JL (2004) Phytoplankton community growth-rate response to nutrient pulses in a shallow turbid estuary, Galveston Bay, Texas. J Plankton Res 26:325–339

Pinckney JL, Paerl HW, Harrington MB (1999) Response of the phytoplankton community growth rate to nutrient pulses in variable estuarine environments. J Phycol 35: 1455–1463

Reckermann M, Veldhuis MJW (1997) Trophic interactions between picophytoplankton and micro- and nanozooplankton in the western Arabian Sea during the NE monsoon 1993. Aquat Microb Ecol 12:263–273

Ringuet S, Mackenzie FT (2005) Controls on nutrient and phytoplankton dynamics during normal flow and storm runoff conditions, southern Kāne'ohe Bay, Hawai'i. Estuaries 28:327–337

Saiz E, Griffell K, Calbet A, Isari S (2014) Feeding rates and prey: predator size ratios of the nauplii and adult females of the marine cyclopoid copepod *Oithona davisae.* Limnol Oceanogr 59:2077–2088

Scheinberg RD, Landry MR, Calbet A (2005) Grazing of two common appendicularians on the natural prey assemblage of a tropical coastal ecosystem. Mar Ecol Prog Ser 294:201–212

Schmoker C, Hernandez-Leon S, Calbet A (2013) Microzooplankton grazing in the oceans: impacts, data variability, knowledge gaps and future directions. J Plankton Res 35:691–706

Selph KE, Shacat J, Landry ML (2005) Microbial community composition and growth rates in the NW Pacific during spring 2002. Geochem Geophys Geosyst 6: Q12M05

Sherr EB, Sherr BF (1993) Preservation and storage of samples for enumeration of heterotrophic protists. In: Kemp PF, Sherr BF, Sherr EB, Cole JJ (eds) Handbook of meth-

ods in aquatic microbial ecology. Lewis Publishers, Boca Raton, FL, p 207–212

Sherr EB, Sherr BF (2002) Significance of predation by protists in aquatic microbial food webs. Antonie Leeuwenhoek 81:293–308

Smith SV, Kimmerer WJ, Laws EA, Brock RE, Walsh TW (1981) Kāne'ohe Bay sewage diversion experiment: perspectives on ecosystem responses to nutritional perturbation. Pac Sci 35:279–395

Stimson J (2015) Long-term record of nutrient concentrations in Kāne'ohe Bay, O'ahu, Hawai'i, and its relevance to onset and end of a phase shift involving an indigenous alga, *Dictyosphaeria cavernosa.* Pac Sci 69:319–339

Stoecker DK, Silver MW, Michaels AE, Davis LH (1988) Obligate mixotrophy in *Laboea strobila*, a ciliate which retains chloroplasts. Mar Biol 99:415–423

Strom SL, Macri EL, Olson MB (2007) Microzooplankton grazing in the Gulf of Alaska: variations in top-down control of phytoplankton. Limnol Oceanogr 52: 1480–1494

Taguchi S, Laws EA (1987) Patterns and causes of temporal variability in the physiological condition of the phytoplankton community in Kāne'ohe Bay, Hawai'i. J Plankton Res 9:1143–1157

Taguchi S, Laws EA (1989) Biomass and compositional characteristics of Kāne'ohe Bay, O'ahu, Hawai'i, phytoplankton inferred from regression analysis. Pac Sci 43: 316–331

Throndsen J (1978) Preservation and storage. In: Sournia A (ed) Phytoplankton manual. UNESCO, Paris, p 69–74

Verity PG (1988) Chemosensory behavior in marine planktonic ciliates. Bull Mar Sci 43:772–782

Verity PG (1991) Measurement and simulation of prey uptake by marine planktonic ciliates fed plastidic and aplastidic nanoplankton. Limnol Oceanogr 36:729–750

Vogt RA, Ignoffo TR, Sullivan LJ, Herndon J, Stillman JH, Kimmerer WJ (2013) Feeding capabilities and limitations in the nauplii of two pelagic estuarine copepods, *Pseudodiaptomus marinus* and *Oithona davisae.* Limnol Oceanogr 58:2145–2157

Welschmeyer NA (1994) Fluorometric analysis of chlorophyll *a* in the presence of chlorophyll *b* and pheopigments. Limnol Oceanogr 39:1985–1992

Worden AZ, Nolan JK, Palenik B (2004) Assessing the dynamics and ecology of marine picophytoplankton: the importance of the eukaryotic component. Limnol Oceanogr 49:168–179

Yeo SK, Huggett MJ, Eiler A, Rappé MS (2013) Coastal bacterioplankton community dynamics in response to a natural disturbance. PLOS ONE 8:e56207

Editorial responsibility: Toshi Nagata, Kashiwanoha, Japan

Submitted: August 10, 2017; Accepted: November 23, 2017
Proofs received from author(s): February 22, 2018